RESEARCH ARTICLE | JANUARY 07 2021

Local coercivity at X-ray nanobeam irradiated regions in amorphous $Fe_{80}B_{20}$ stripes

U. Urdiroz; E. Navarro; M. Sánchez-Agudo; F. Cebollada ; F. J. Palomares; G. Martínez Criado; J. M. González

AIP Advances 11, 015318 (2021)
https://doi.org/10.1063/9.0000090

Local coercivity at X-ray nanobeam irradiated regions in amorphous $Fe_{80}B_{20}$ stripes

Cite as: AIP Advances 11, 015318 (2021); doi: 10.1063/9.0000090
Presented: 4 November 2019 • Submitted: 14 October 2020 •
Accepted: 16 November 2020 • Published Online: 7 January 2021

U. Urdiroz,[1,2] E. Navarro,[1] M. Sánchez-Agudo,[2] F. Cebollada,[2] F. J. Palomares,[1] G. Martínez Criado,[1] and J. M. González[1,a)]

AFFILIATIONS

[1] Instituto de Ciencia de Materiales de Madrid (ICMM), A.E. Consejo Superior de Investigaciones Científicas (CSIC), 28049 Madrid, Spain

[2] POEMMA-CEMDATIC, Escuela Técnica Superior de Ingenieros de Telecomunicación-Universidad Politécnica de Madrid, 28040 Madrid, Spain

Note: This paper was presented at the 65th Annual Conference on Magnetism and Magnetic Materials.
[a)] **Author to whom correspondence should be addressed:** jm.g@csic.es

ABSTRACT

We report on the effect, on the local magnetization reversal taking place in amorphous $Fe_{80}B_{20}$ stripes, of the irradiation with nanobeam synchrotron X-ray. That irradiation preserves the amorphous structure and results on the increase of the local coercivity with respect to that measured in a non-irradiated sample, in which the coercivity is mediated by the nucleation-propagation of a single wall. The local coercivity increases in a non-linear way with the width of the irradiated regions when that width is smaller than that of the wall mediating the magnetization switching in the non-irradiated stripe and gets saturated when the irradiated regions dimension is larger than the propagating wall width. We correlate this behavior with the induction at the irradiated regions of a reduction of the local effective anisotropy with respect to the stripe as-lithographed value. From the relationship between the coercivity and the width of the irradiated regions we estimate the local anisotropy reduction in a 25% of that measured in the non-irradiated stripe.

INTRODUCTION

Ferromagnetic metallic amorphous systems are characterized by the possibility of modifying their effective anisotropy[1] due to their metastable nature that favors the occurrence of atomic diffusion.[2] Thermal treatments carried out at temperatures significantly below the crystallization onset result on a reduction of the as-prepared material built-in anisotropy, which can be associated to structural relaxation/free volume elimination and/or stresses relief.[3] When the treatments are performed at temperatures closer to the crystallization onset, while keeping the samples submitted to diffusion polarizing magnetic and/or stress fields, it is possible to induce controlled easy axis direction anisotropies with constants of the order of 1-5 x 10^4 erg/cm^3.[4–6] In the particular case of the amorphous magnetic films, the induction of anisotropy at the local scale has been implemented by using a variety of techniques including ion implantation,[7–10] electromagnetic irradiation,[11] coupling to locally strained regions,[12] and local anneals carried out by means of current circulating through auxiliary conducting tracks.[13] In a previous paper[14] the authors have shown how irradiating with synchrotron X-ray (2 μm sized beam) the same amorphous $Fe_{80}B_{20}$ stripes studied here results on anisotropy modifications over regions spanning ca. 15 μm.

In the present work we explore the local anisotropy changes induced in amorphous $Fe_{80}B_{20}$ stripes by means of nanosized X-ray beams since that length scale is of special interest from the standpoint of the implementation of spin waves-based devices and circuitry of the types proposed to implement processing components (i.e.: logic gates[14,15]).

SAMPLES AND EXPERIMENTAL

The measured stripes (750 μm long and 15 μm wide) were prepared by maskless laser lithography from precursor 15 nm thick $Fe_{80}B_{20}$ films deposited by means of a UHV Pulsed Laser Ablation

device onto MgO(001) substrates. The crystallinity of the precursor films, lithographed stripes and irradiated regions (IRs) was checked by means of X-ray diffraction (XRD). The irradiation was performed at the Nano-Analysis line ID16B of the ESRF (Grenoble), by using a 60 nm x 60 nm spot, a maximum of the energy at E = 17.5 keV with $\Delta E/E = 10^{-2}$ and a flux of 2.21 x 10^{11} photons/s. The stripes were irradiated by scanning the beam along a direction perpendicular to the stripe long axis during a total time of 540 s. For irradiating regions with widths larger than 60 nm, the beam was displaced along the stripe axis (in 60 nm steps) to perform transverse scans along lines parallel and contiguous to the previously irradiated ones until reaching the required nominal width. The local hysteretic behavior of the stripes was measured before and upon irradiation by using a magnetometric magneto-optic Kerr effect (MOKE) device with a 20 μm spot, displaceable along the stripe. We measured the in-plane component of the magnetization parallel to the applied field direction.

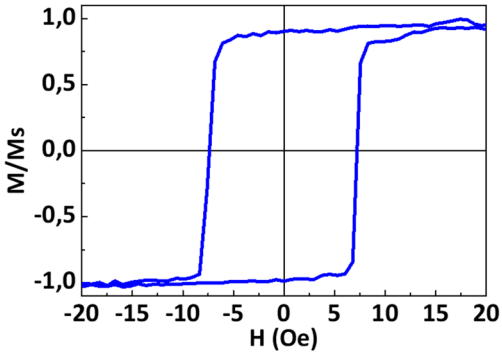

FIG. 1. MOKE Hysteresis loop measured along the stripe long axis (e.a.) in a non-irradiated sample.

RESULTS AND DISCUSSION

The as-deposited precursor films, lithographed stripes and IRs were XRD amorphous down to the technique resolution. Upon annealing the precursor films at temperatures of the order of 150 °C (isothermal, 60 minutes treatment with rapid heating and cooling) they experienced structural relaxation. That relaxation was identified from the high X-ray intensity, low angle XRD diffractograms in which a clear angular displacement of the amorphous hump with respect to its as-deposited angular position was detected (without observing any crystalline peak). The onset of the crystallization, identified through the detection of high angle peaks, took place upon annealing the films at 250 °C.

The as-lithographed stripes exhibited shape anisotropy with easy axis (e.a.) along the stripe long axis and a square hysteresis loop was measured along that direction, see Figure 1. In a previous work on the same stripes that included MOKE microscopy results,[14] the non-irradiated stripe magnetization reversal was characterized in detail. It started at one of the stripe ends by the nucleation of a wall (favored by the local occurrence at the stripe end corners of large demagnetizing fields[16]). After nucleation the demagnetizing field increase resulted on the propagation of the wall that swept the stripe with only marginal pinning at some morphological defects present at the stripe lateral sides. Globally, the nucleation-propagation sequence originated a coercivity of 8 Oe (Figure 1). From the measurement of the (anhysteretic) hysteresis loop in the transverse-to-the-stripe axis direction and the stripe magnetometric saturation magnetization value, M_S = 1.44 x 10^4 Oe,[14] the corresponding anisotropy constant was evaluated in 1.0 x 10^4 erg/cm^3.

In Figure 2 a sketch (not to scale) illustrating the IRs positions and dimensions is shown. Five different IRs, with the indicated widths and separated by 100 μm, were prepared by means of the synchrotron nanobeam. The effect on the local hysteresis of the irradiation was followed by positioning the MOKE spot at all the regions in between two consecutive IRs and beyond the IR having a width of 1440 nm.

In Figure 3 we have plotted the demagnetization branches measured along the e.a. direction at all the considered MOKE positions. The procedure followed to measure those branches started (after positioning the MOKE spot at the measurement site) by saturating the stripe in the sense indicated in Figure 2 and then taking the applied field to zero, switching it and increasing the demagnetizing field (sense indicated in Figure 2) up to reach the saturation opposite to the initial one. Along this demagnetization process, similarly to that discussed in Ref. 14 for a non-irradiated stripe, a wall was nucleated at the left stripe end in Figure 2 due to the local demagnetizing fields. The stripe ends are 150 μm distant from the closer IR and, consequently do not experience any anisotropy modification during the irradiation process.[14] This should result on nucleation-propagation fields similar to those measured in the non-irradiated

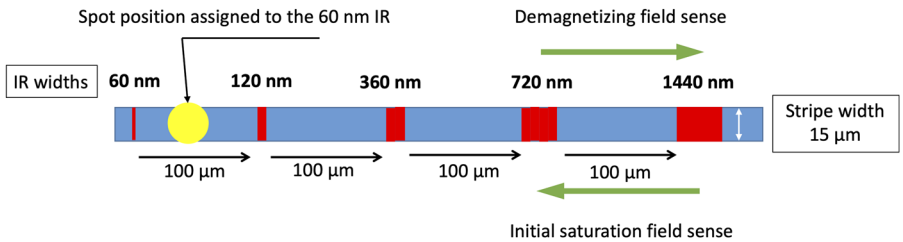

FIG. 2. Sketch (not to scale) displaying the widths and distances between the IRs (shown in red) prepared in a $Fe_{80}B_{20}$ stripe (shown in blue). As an example of the MOKE spot positions used to measure the local demagnetization, a spot having a diameter of 20 μm and placed in between the 60 nm and the 120 nm IRs is shown in yellow (the spot position is assigned to the IR in the pair having the smaller width, i.e.: 60 nm in the considered case). The green arrows identify the initial saturation sense as well as that corresponding to the applied demagnetizing field.

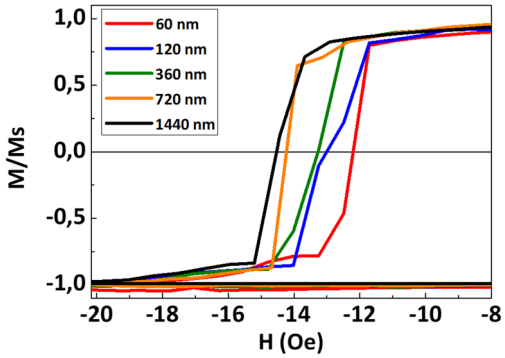

FIG. 3. Demagnetization branches measured along the e.a. by placing the spot at all the different positions in between two consecutive IRs. The curves are labelled with the smaller width of the IRs pairs in between of which the spot was positioned.

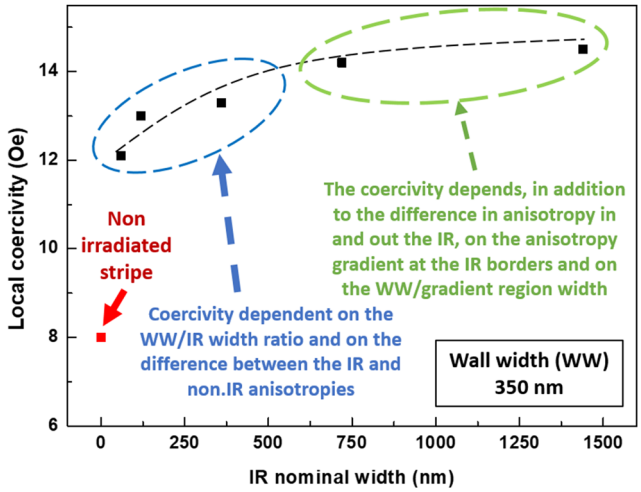

FIG. 4. IR width dependence of the local coercivity measured by positioning the MOKE spot in between the different pairs of IRs (the non-irradiated stripe coercivity is also plotted for the sake of comparison). Each coercivity value was associated to the IR having the smaller width of the pair.

sample. Once the nucleated wall propagates, it sweeps the stripe finding the IRs in increasing IR width order. At every MOKE spot position in between a pair of IRs (distant 100 μm) we observe (Figure 3) that the local demagnetization process occurs at fields that are larger than the non-irradiated coercivity and that monotonically increase with the IR width. From these results we conclude that the propagating wall gets sequentially pinned at the IRs it finds when moving towards the stripe end on the right side in Figure 2, and that the coercivities of the local demagnetization branches give a measure of the depinning fields associated to the IRs having the smaller width of the pairs in between of which the spot is located. Once the wall is depinned from a given IR it sweeps the region separating that IR from the next one in the sequence in Figure 2 and in that process it is detected by our MOKE spot. The wall gets pinned again when it reaches the IR having the larger width in the considered IRs pair.

In the IR widths range from 60 nm up to 360 nm (Figure 4), the local depinning field markedly increases with the increase of the IR width from the non-irradiated stripe value. Above 360 nm the depinning field gets nearly IR width independent. We associate the origin of the pinning effect to a local decrease, at the IR, of the effective anisotropy induced by the X-ray nanobeam, that could result from a local increase of the temperature during the irradiation of the order of that linked to the induction of structural relaxation (ca. 150 °C). The mechanism of effective anisotropy reduction could correspond either to the local elimination of internal stresses[17] or to the induction of a transverse e.a. (similarly to the behavior observed in Ref. 14) whose absolute magnitude should be lower than that of the e.a. present in the non-irradiated sample to result in an effective longitudinal e.a.

The measured demagnetization branches coercivity values, being associated to depinning processes, correspond to the difference in energies between those of the propagating wall at the pinned and depinned states, the latter one being identifiable with the wall energy in a non-irradiated stripe. The wall energy at the pinned state depends on the pinned wall structure and, consequently, on the wall/IR widths ratio, and possibly on the homogeneity of the induced anisotropy near the IR.[14] Considering the anisotropy constant measured in the non-irradiated stripe (1.0×10^4 erg/cm^3) and an exchange constant of 10^{-6} erg/cm we estimate the domain wall width in that sample in 350 nm and we will assume that the wall has that approximate thickness both when it is pinned and when it propagates. Taking into account the local coercivity at the IR having a width of 360 nm (13.2 Oe) and the stripe saturation magnetization value, $M_S = 1.44 \times 10^4$ Oe,[14] we estimate the local anisotropy at the 360 nm IR in 7.6×10^3 erg/cm. At the large IR width range the pinned wall has a smaller width than that of the pinning IR. In this range the energy of the pinned wall is independent of the IR width and consequently the coercivity does not significantly vary with that parameter. Despite this, for large IR widths, the depinning field value is not exclusively related to the anisotropy difference between the wall inside the IR and outside of it. This is so due to the fact that both the anisotropy constant gradient at the borders of the IR and the relative sizes of that gradient region and the wall width influence the depinning field.[5] If it is assumed, in the case of the 1440 nm IR, that the anisotropy decreases in an infinite slope step at both IR borders (I,e.: that the coercivity depends exclusively on the anisotropy difference between the iR and the non-irradiated region) a value for the local effective anisotropy of 6.9×10^3 erg/cm is obtained.

To conclude, we have shown that the nanobeam irradiation of amorphous $Fe_{80}B_{20}$ stripes results in a local effective anisotropy modification that originates pinning centers for the wall movement. Through the variation of the local depinning field with the IR width, we have estimated that local modification as corresponding to a moderate anisotropy decrease.

ACKNOWLEDGMENTS

This work has been developed with funds corresponding to project MAT2016-80394-R financed by the Spanish Research Agency (AEI) and 2019AEP150 by A.E. Consejo Superior de Investigaciones Científicas (CSIC). We also acknowledge the Spanish

Ministerio de Ciencia e Innovación and Consejo Superior de Investigaciones Científicas for financial support and for provision of synchrotron radiation at beamline BM25-SpLine (ESRF). U.U. acknowledges FPI grant BES-2014-070387.

DATA AVAILABILITY

The data that support the findings of this study are available from the corresponding author upon reasonable request.

REFERENCES

[1]P. R. Ohodnicki, J. Long, D. E. Laughlin, M. E. McHenry, V. Keylin, and J. Huth, "Composition dependence of field induced anisotropy in ferromagnetic $(Co,Fe)_{89}Zr_7B_4$ and $(Co,Fe)_{88}Zr_7B_4Cu_1$ amorphous and nanocrystalline ribbons," Journal of Applied Physics **104**, 113909 (2008).

[2]C. C. Tsuei and P. Duwez, "Metastable Amorphous ferromagnetic phases in palladium-base alloys," Journal of Applied Physics **37**, 435 (1966).

[3]J. Bork, "Investigation of the structural relaxation in amorphous metals by ferromagnetic resonance with spin exchange," Journal of Magnetism and Magnetic Materials **26**(1–3), 143–146 (1982).

[4]F. Luborsky and J. Walter, "Magnetic anneal anisotropy in amorphous alloys," IEEE Trans. Magn. **13**(2), 953–956 (1977).

[5]N. Murillo, J. M. Blanco, J. González, J. M. González, and T. Kulik, "Stress annealing in $Fe_{73.5}Cu_1Ta_3Si_{13.5}B_9$ amorphous alloy: Induced magnetic anisotropy and variation of the magnetostriction constant," Journal of Applied Physics **76**(2), 1131–1134 (1994).

[6]O. V. Nielsen, A. Hernando, V. Madurga, and J. M. Gonzalez, "Experiments concerning the origin of stress anneals induced magnetic anisotropy in metallic glass ribbons," J. Magn. Magn. Mater. **46**(3), 341–349 (1985).

[7]J. Fassbender and J. McCord, "Magnetic patterning by means of ion irradiation and Implantation," J. Magn. Magn. Mater. **320**(3–4), 579–596 (2008).

[8]W. Rupp *et al.*, "Ion-beam induced fcc-bcc transition in ultrathin Fe films for ferromagnetic patterning," Appl. Phys. Lett. **93**(6), 063102 (2008).

[9]J. Gloss *et al.*, "Ion-beam-induced magnetic and structural phase transformation of Ni-stabilized face-centered-cubic Fe films on Cu (100)," Appl. Phys. Lett. **103**(26), 262405 (2013).

[10]M. Urbánek *et al.*, "Research Update: Focused ion beam direct writing of magnetic patterns with controlled structural and magnetic properties," APL Mater. **6**(6), 060701 (2018).

[11]M. Sorescu, E. T. Knobbe, D. Barb, D. Sorescu, and I. Bibicu, "Comparison of electron beam and pulsed laser irradiation effects in $Fe_{80}B_{20}$," Hyperfine Interact. **92**(1), 1347–1353 (1994).

[12]P. Corte-León *et al.*, "Engineering of magnetic softness and domain wall dynamics of Fe-rich amorphous microwires by stress-induced magnetic anisotropy," Sci. Rep. **9**(1), 1–14 (2019).

[13]C. Moron, A. García, M. T. Carracedo, and F. Maganto, "Domain structure of local current annealed amorphous ribbons," Journal of Materials Processing Technology **143-144**, 130–133 (2003).

[14]U. Urdiroz *et al.*, "Antiphase resonance at x-ray irradiated microregions in amorphous $Fe_{80}B_{20}$ stripes," Journal of Magnetism and Magnetic Materials **520**, 167017 (2020).

[15]A. Khitun, M. Bao, and K. L. Wang, "Magnonic logic circuits," Journal of Physics D: Applied Physics **43**(26), 264005 (2010).

[16]A. Smith, K. K. Nielsen, D. V. Christensen, C. R. H. Bahl, R. Bjørk, and J. Hattel, "The demagnetizing field of a nonuniform rectangular prism," Journal of Applied Physics **107**, 103910 (2010).

[17]N. Pompeo, A. Alimenti, K. Torokhtii, E. Bartolomé, A. Palau, T. Puig, A. Augieri, V. Galluzzi, A. Mancini, G. Celentano, X. Obradors, and E. Silva, "Intrinsic anisotropy and pinning anisotropy in nanostructured YBa2Cu3O7−δ from microwave measurements," arXiv:2001.10299 [cond-mat.supr-con].